



HAL
open science

Mathematical study of a two-stage anaerobic model when the hydrolysis is the limiting step

Mohammed Hanaki, Jérôme Harmand, Zoubida Mghazli, Tewfik Sari, Alain Rapaport, Pablo Ugalde

► **To cite this version:**

Mohammed Hanaki, Jérôme Harmand, Zoubida Mghazli, Tewfik Sari, Alain Rapaport, et al.. Mathematical study of a two-stage anaerobic model when the hydrolysis is the limiting step. 2020. hal-02531141v2

HAL Id: hal-02531141

<https://hal.science/hal-02531141v2>

Preprint submitted on 6 Apr 2020

HAL is a multi-disciplinary open access archive for the deposit and dissemination of scientific research documents, whether they are published or not. The documents may come from teaching and research institutions in France or abroad, or from public or private research centers.

L'archive ouverte pluridisciplinaire **HAL**, est destinée au dépôt et à la diffusion de documents scientifiques de niveau recherche, publiés ou non, émanant des établissements d'enseignement et de recherche français ou étrangers, des laboratoires publics ou privés.

Mathematical study of a two-stage anaerobic model when the hydrolysis is the limiting step

Mohammed Hanaki^{a,*}, Jérôme Harmand^b, Zoubida Mghazli^a, Tewfik Sari^c, Alain Rapaport^d, Pablo Ugalde^b

^a*LIRNE, Ibn Tofail University, Kenitra, Morocco*

mohammed.hanaki@uit.ac.ma

zoubida.mghazli@uit.ac.ma

^b*LBE, University of Montpellier, INRAE, Narbonne, France*

jerome.harmand@inrae.fr

pablo.ugalde-salas@inrae.fr

^c*ITAP, University of Montpellier, INRAE, Montpellier SupAgro, Montpellier, France*

tewfik.sari@inrae.fr

^d*MISTEA, University of Montpellier, INRAE, Montpellier SupAgro, Montpellier, France*

alain.rapaport@inrae.fr

Abstract

We study mathematically and numerically a 2-step model of anaerobic digestion process. We focus on the hydrolysis and methanogenesis phases when applied to the digestion of waste with a high content in solid matter: existence and stability properties of the equilibrium points are investigated. The hydrolysis step is considered as a limiting step in this process using the Contois growth function for the bacteria responsible for the first degradation step. The methanogenesis step being inhibited by the product of the first reaction (which is also the substrate for the second one), the Haldane growth rate is used for the second reaction step. The operating diagrams with respect to the dilution rate and the input substrate concentrations are established and discussed.

Keywords: Anaerobic digestion, Steady state, Mortality, Stability, Operating diagrams.

1. Introduction

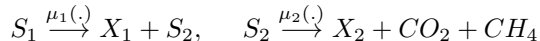
Anaerobic digestion is the degradation of organic matter in the absence of oxygen. The final product being methane, a renewable energy. This process is more and more used for the treatment of liquid and solid waste. Because of its relative instability due to the possible accumulation of intermediate products, notably the volatile fatty acids (VFA), the modeling of this process has been extensively studied over these last years. Such models are multi-step mass balance models in which the reactional network consists in a number of biological reactions taking place the medium in parallel and / or in series. Their complexity highly depends on the objectives by the modeler. On the one hand, when the objective is to develop models for integrating and formalize the available knowledge typically to better understand bioprocesses, models are generally high order models and not tractable from a mathematical viewpoint, cf. for instance the ADM1 [1]. On the other hand, when the aim of the modeling is to develop decision tools or control systems, low order models are better suited, as for instance the AM2 [3]. In this second class of

*Corresponding author

Email address: hanaki.mohammed@gmail.com (Mohammed Hanaki)

models, several two-steps models have been proposed in the literature.

Two steps models are commonly used to describe commensalistic microbial systems which take the form of a cascade of two biological reactions where one substrate S_1 is consumed by one microorganism/ecosystem X_1 to produce S_2 which serves as the main limiting substrate for a second microorganism/ecosystem X_2 as schematically represented by the following reaction scheme representing a simplified scheme of the anaerobic digestion



The most general two-step model under interest in the actual paper can be written as :

$$\begin{cases} \dot{S}_1 = D(S_1^{in} - S_1) - \mu_1(\cdot) \frac{X_1}{Y_1}, \\ \dot{X}_1 = [\mu_1(\cdot) - \alpha D - k_1] X_1, \\ \dot{S}_2 = D(S_2^{in} - S_2) + \mu_1(\cdot) \frac{X_1}{Y_3} - \mu_2(\cdot) \frac{X_2}{Y_2}, \\ \dot{X}_2 = [\mu_2(\cdot) - \alpha D - k_2] X_2 \end{cases} \quad (1)$$

where D is the dilution rate, while S_1^{in} and S_2^{in} are the input substrate concentrations respectively. Parameters Y_i are yield coefficients associated to the bioreactions, k_i are the mortality terms while $\alpha \in [0, 1]$ is a term allowing to decouple the retention time applying on substrates (supposed to be soluble) and biomass (supposed to be particulate). The kinetics μ_1 and μ_2 are of Contois and Haldane type. By Contois or Haldane-"type", we mean functions that are defined by qualitative properties. For μ_1 , it means a density dependant function which is increasing with S_1 but decreasing with X_1 while μ_2 is non monotonic (cf. modeling hypotheses in the next section).

The different analyses of the class of models (1) available in the literature essentially differ on the way the growth rate functions are characterized and whether a specific input for S_2 is considered or not (i.e., the presence of a term S_2^{in} in the dynamic equation of S_2). They differ also in the presence or not i) of a coefficient α allowing to decouple the solid and liquid retention times and ii) of a maintenance term $k_i(\cdot)$. For details and informations on the various models considered in the existing literature the reader can refer to [9], or Table (2) and Table (3) in the review paper [13].

A first mathematical study of a pure commensalistic model was proposed by Reilly [7], where $\mu_1 : S_1 \mapsto \mu_1(S_1)$, $\mu_2 : S_2 \mapsto \mu_2(S_2)$, $k_1 = k_2 = 0$, $\alpha = 1$ and some extensions. He was interested at explaining surprising oscillations observed during an experiment realized in making *Saccharomyces carlsbergensis* growing on fructose produced by *Acetobacter suboxyduns* from mannitol. In particular, he established theoretical conditions involving an interval feedback from the yeast to the bacteria. For more information on commensalism, the reader can refer to Stephanopoulos [10]. An important contribution on the modeling of anaerobic digestion as a commensalistic system is the model by Bernard et al. [3]. The authors considered a Monod function for μ_1 and a Haldane function for μ_2 . Sbarciog and al. [8] studied this model for $\alpha = 1$ while the most interesting case where $0 < \alpha < 1$ and where growth functions were characterized by qualitative properties was studied in [2].

Depending on the nature of treated waste, the limiting step of anaerobic digestion is not the same. If treated waste is liquid, the main limiting step usually considered to be the methanogenesis: in such a case, simple models including only

acidogenesis and methanogenesis can be used (cf. for instance Bernard et al. [3]). If the waste contains a high proportion of solid matter, it is the rule rather than the exception to consider that the hydrolysis which is the main limiting step and a model including only hydrolysis and methanogenesis can be used. However, as proposed in Vavilin, [11], when hydrolysis is the limiting step, rates depending only on substrate concentrations, such as Monod model, are not the most appropriate. It is better to describe such complex phenomena by density-dependent models, such as density dependent kinetics, a family in which Contois models falls. Contois model. Using this model, the rate of the hydrolysis step is modeled as :

$$\mu_1(S_1, X_1) = \frac{m_1 S_1}{K_1 X_1 + S_1} = \frac{m_1 \frac{S_1}{X_1}}{K_1 + \frac{S_1}{X_1}}$$

which exhibits the following properties specific to hydrolysis (cf. Mottet et al. [6])

$$\begin{cases} \frac{S_1}{X_1} \gg K_1 \Rightarrow \mu_1(S_1, X_1) X_1 \approx m_1 X_1 \propto X_1, \\ \frac{S_1}{X_1} \ll K_1 \Rightarrow \mu_1(S_1, X_1) X_1 \approx \frac{m_1}{K_1} S_1 \propto S_1 \end{cases} \quad (2)$$

While the analysis of the general model of anaerobic digestion initially purposed by Bernard et al., [3] (representing acidogenesis and methanogenesis steps) has been realized by Benyahia et al., [2], from the best of authors knowledge, a two-step model where the kinetic of the first step is modeled by a density-dependent kinetics while the second step exhibits a "Haldane-type" function has never been studied in the literature. It is the aim of the actual paper to study such a generic model.

The paper is organized as follows. In section 2 we present the two-step model with two input substrate concentrations and we give the general hypotheses on the growth functions. In section 3 we give the expressions of the steady states and in section 4, we discuss their stability. In section 5, we illustrate the effect of the second input substrate concentration on the steady states, in designing the operating diagrams, first, with respect to the first input substrate concentration and the dilution rate and second, with respect to the second input substrate concentration and the dilution rate.

1.1. Mathematical model

The two-step model reads:

$$\begin{cases} \dot{S}_1 = D(S_1^{in} - S_1) - \mu_1(S_1, X_1) \frac{X_1}{Y_1}, \\ \dot{X}_1 = [\mu_1(S_1, X_1) - D_1] X_1, \\ \dot{S}_2 = D(S_2^{in} - S_2) + \mu_1(S_1, X_1) \frac{X_1}{Y_3} - \mu_2(S_2) \frac{X_2}{Y_2}, \\ \dot{X}_2 = [\mu_2(S_2) - D_2] X_2 \end{cases} \quad (3)$$

where S_1 and S_2 are the substrate concentrations introduced in the chemostat with input concentrations S_1^{in} and S_2^{in} . $D_1 = \alpha D + k_1$ and $D_2 = \alpha D + k_2$, where D is the dilution rate, k_1 and k_2 represent maintenance terms and parameter $\alpha \in [0, 1]$ represents the fraction of the biomass affected by the dilution rate while Y_i are the yield coefficients. X_1 and X_2 are the hydrolytic bacteria and methanogenic bacteria concentrations. The functions $\mu_1 : (S_1, X_1) \rightarrow \mu_1(S_1, X_1)$ and $\mu_2 : (S_2) \rightarrow \mu_2(S_2)$

are the specific growth rates of the bacteria.

To ease the mathematical analysis of the system, we can rescale system (3). Notice that it is simply equivalent to changing units of variables:

$$s_1 = S_1, \quad x_1 = \frac{1}{Y_1} X_1, \quad s_2 = \frac{Y_3}{Y_1} S_2, \quad x_2 = \frac{Y_3}{Y_1 Y_2} X_2$$

We obtain the following system

$$\begin{cases} \dot{s}_1 = D(s_1^{in} - s_1) - f_1(s_1, x_1)x_1, \\ \dot{x}_1 = [f_1(s_1, x_1) - D_1]x_1, \\ \dot{s}_2 = D(s_2^{in} - s_2) + f_1(s_1, x_1)x_1 - f_2(s_2)x_2, \\ \dot{x}_2 = [f_2(s_2) - D_2]x_2 \end{cases} \quad (4)$$

Where $s_2^{in} = \frac{Y_3}{Y_1} S_2^{in}$ and f_1 and f_2 are defined by

$$f_1(s_1, x_1) = \mu_1(s_1, Y_1 x_1) \quad \text{and} \quad f_2(s_2) = \mu_2\left(\frac{Y_1}{Y_3} s_2\right)$$

We assume that the functions $\mu_1(., .)$ and $\mu_2(.)$ satisfy :

H1. $\mu_1(s_1, x_1)$ is positive for $s_1 > 0$, $x_1 > 0$, and satisfies $\mu_1(0, x_1) = 0$ and $\mu_1(+\infty, x_1) = m_1(x_1)$. Moreover $\mu_1(s_1, x_1)$ is strictly increasing in s_1 , and decreasing in x_1 that is to say $\frac{\partial \mu_1}{\partial s_1} > 0$ and $\frac{\partial \mu_1}{\partial x_1} \leq 0$ for $s_1 > 0$, $x_1 > 0$.

H2. $\mu_2(s_2)$ is positive for $s_2 > 0$, and satisfies $\mu_2(0) = 0$ and $\mu_2(+\infty) = 0$. Moreover $\mu_2(s_2)$ increases until a concentration s_2^M and then decreases, with $\mu_2'(s_2) > 0$ for $0 \leq s_2 < s_2^M$, and $\mu_2'(s_2) < 0$ for $s_2 > s_2^M$.

As underlined in the introduction, particular kinetics models as Contois function verifies **H1** while Haldane function verifies **H2**.

Since the functions μ_1 and μ_2 satisfy the hypotheses **H1** and **H2**, it follows from the above that functions f_1 and f_2 satisfy :

A1. $f_1(s_1, x_1)$ is positive for $s_1 > 0$, $x_1 > 0$, and satisfies $f_1(0, x_1) = 0$ and $f_1(+\infty, x_1) = m_1(x_1)$. Moreover $\frac{\partial f_1}{\partial s_1} > 0$ and $\frac{\partial f_1}{\partial x_1} \leq 0$ for $s_1 > 0$, $x_1 > 0$.

A2. $f_2(s_2)$ is positive for $s_2 > 0$, and satisfies $f_2(0) = 0$ and $f_2(+\infty) = 0$. Moreover $f_2(s_2)$ increases until a concentration s_2^M and then decreases, with $f_2'(s_2) > 0$ for $0 < s_2 < s_2^M$, and $f_2'(s_2) < 0$ for $s_2 > s_2^M$.

2. Analysis of the model

2.1. The dynamics of s_1 and x_1

Model (4) has a cascade structure which renders its analysis easier. In other terms s_1 and x_1 are not influenced by variables s_2 and x_2 and their dynamics is given by:

$$\begin{cases} \dot{s}_1 = D(s_1^{in} - s_1) - f_1(s_1, x_1)x_1, \\ \dot{x}_1 = [f_1(s_1, x_1) - D_1]x_1. \end{cases} \quad (5)$$

The behavior of this system is well-know, see [4]. A steady state (s_1^*, x_1^*) must be solution of the system

$$\begin{cases} 0 = D(s_1^{in} - s_1) - f_1(s_1, x_1)x_1, \\ 0 = [f_1(s_1, x_1) - D_1]x_1 \end{cases} \quad (6)$$

From the second equation we deduce that $x_1^* = 0$, which corresponds to the washout $E_0 = (s_1^{in}, 0)$, or s_1^* and x_1^* must satisfy both equations

$$f_1(s_1^*, x_1^*) = D_1 \quad \text{and} \quad x_1^* = \frac{D}{D_1}(s_1^{in} - s_1^*). \quad (7)$$

Let γ a function defined by :

$$\gamma(s_1) = f_1\left(s_1, \frac{D}{D_1}(s_1^{in} - s_1)\right),$$

so s_1^* is a solution of $\gamma(s_1) = D_1$, and we notice that $\gamma'(s_1) = \frac{\partial f_1}{\partial s_1} - \frac{D}{D_1} \frac{\partial f_1}{\partial x_1}$. According to the hypothesis **A1**, $\gamma(s_1)$ is strictly increasing over the interval $]0, s_1^{in}[$, with $\gamma(0) = 0$ and $\gamma(s_1^{in}) = f_1(s_1^{in}, 0)$. According to the theorem of intermediate values, the equation $\gamma(s_1) = D_1$ has a solution between 0 and s_1^{in} if and only if $D_1 < \gamma(s_1^{in})$, that is to say if $D_1 < f_1(s_1^{in}, 0)$ (See Fig. (1)).

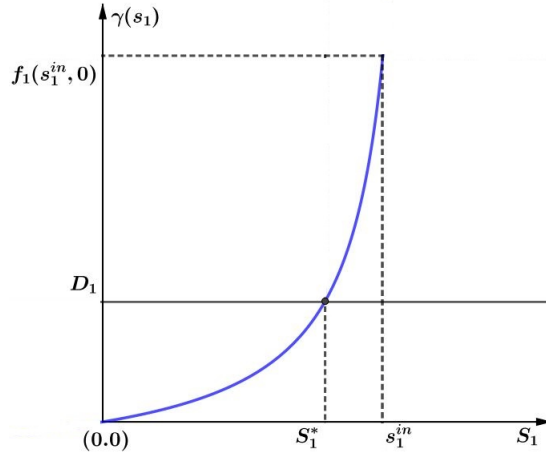


Figure 1: The existence of the solution of $\gamma(s_1) = D_1$.

Hence, for $x_1^* \neq 0$, the equilibrium $E_1(s_1^*, x_1^*)$ exists if and only if $D_1 < f_1(s_1^{in}, 0)$. The local stability of the steady state is given by the sign of the real part of eigenvalues of the Jacobian matrix. In the following, we use the abbreviations LES for locally exponentially stable.

Proposition 2.1. *Assume that assumptions **A1** and **A2** hold. Then, the local stability of steady states of (5) is given by :*

1. $E_0 = (s_1^{in}, 0)$ is LES if and only if $f_1(s_1^{in}, 0) < D_1$ (i.e. $s_1^{in} < s_1^*$).
2. $E_1 = (s_1^*, x_1^*)$ is LES if and only if $f_1(s_1^{in}, 0) > D_1$ (i.e. $s_1^{in} > s_1^*$), (E_1 is stable if it exists)

When E_0 and E_1 coincide, the equilibrium is attractive (the eigenvalue equal to zero) The results are summarized in the following table :

Steady state	Existence condition	Stability condition
E_0	Always exists	$f_1(s_1^{in}, 0) < D_1$
E_1	$f_1(s_1^{in}, 0) > D_1$	Stable when it exists

Proof

The local stability of (5) of each steady state depends on the sign of the real parts of the eigenvalues of the corresponding Jacobian matrix. At a given steady state (s_1, x_1) , this matrix is given by :

$$J = \begin{bmatrix} -D - Mx_1 & -Nx_1 - f_1(s_1, x_1) \\ Mx_1 & Nx_1 + [f_1(s_1, x_1) - D_1] \end{bmatrix}, \quad (8)$$

where

$$M = \frac{\partial f_1}{\partial s_1}(s_1, x_1), \quad N = \frac{\partial f_1}{\partial x_1}(s_1, x_1).$$

The eigenvalues of J are the roots of its characteristic polynomial $\det(J - \lambda I)$.

- For $E_0 = (s_1^{in}, 0)$, the Jacobian matrix reads

$$J(E_0) = \begin{bmatrix} -D & -f_1(s_1^{in}, 0) \\ 0 & f_1(s_1^{in}, 0) - D_1 \end{bmatrix}.$$

Its eigenvalues are $\lambda_1 = -D$ and $\lambda_2 = f_1(s_1^{in}, 0) - D_1$. For being stable, we need $\lambda_2 < 0$. Therefore, E_0 is stable if and only if

$$f_1(s_1^{in}, 0) < D_1.$$

- For $E_1 = (s_1, x_1)$, where $f_1(s_1, x_1) = D_1$, the Jacobian matrix becomes :

$$J_{E_1} = \begin{bmatrix} -D - Mx_1 & -Nx_1 - D_1 \\ Mx_1 & Nx_1 \end{bmatrix}.$$

As the eigenvalues λ_1 and λ_2 of a square matrix of dimension two are the solutions of the equation

$$\det(J_{E_1} - \lambda I) = \lambda^2 - \text{Tr}J_{E_1}\lambda + \det J_{E_1}, \quad (9)$$

The real parts are strictly negative if and only if $\det A > 0$ and $\text{Tr}A < 0$. Therefore by **A1** we have

$$\det(J_{E_1}) = -DNx_1 + D_1Mx_1 > 0,$$

$$\text{Tr}(J_{E_1}) = -D - Mx_1 + Nx_1 < 0,$$

then E_1 is LES if it exists.

Operating diagram

Apart from the two operating (or control) parameters, which are the input substrate concentration s_1^{in} and the dilution rate D that can vary, all others parameters (α , k_1 and the parameters of the growth function $f_1(s_1, x_1)$) have biological meaning and are fixed depending on the organisms and substrate considered. The operating diagram shows how the system behaves when we vary the two control parameters s_1^{in} and D . The operating diagram is shown in Fig. (2). The condition $f_1(s_1^{in}, 0) > D_1$ of existence of E_1 is equivalent to $D < \frac{1}{\alpha}[f_1(s_1^{in}, 0) - k_1]$. Therefore, the curve

$$\Gamma : \left\{ (s_1^{in}, D) : D = \frac{1}{\alpha}[f_1(s_1^{in}, 0) - k_1] \right\}$$

separates the operating plan in two regions as defined in Fig. (2).

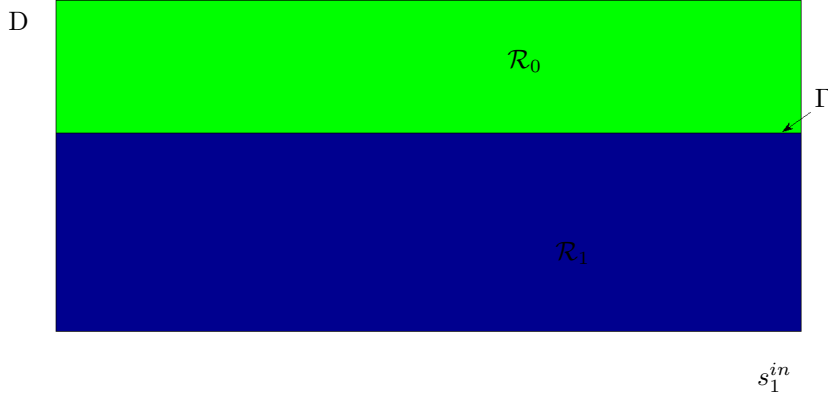


Figure 2: Operating diagram of (5)

The curve Γ is the border which makes E_0 unstable and at the same time E_1 exists. The following table indicates the stability properties of steady state in each region.

region	E_0	E_1
$(s_1^{in}, D) \in \mathcal{R}_0$	S	
$(s_1^{in}, D) \in \mathcal{R}_1$	U	S

Except for small values of D and s_1^{in} , notice that the operating diagram of this first part of the 2-step system under study is qualitatively similar to that one of the first part of the AM2 model (when a Monod-like growth function is considered, cf. [3]).

2.2. The dynamics of s_2 and x_2

Due to the cascade structure of (4), the dynamics of the state variables s_2 and x_2 are given by

$$\begin{cases} \dot{s}_2 = D(F(t) - s_2) - f_2(s_2)x_2, \\ \dot{x}_2 = [f_2(s_2) - D_2]x_2, \end{cases} \quad (10)$$

with

$$F(t) = s_2^{in} + \frac{1}{D}f_1(s_1(t), x_1(t))x_1(t)$$

where $s_1(t), x_1(t)$ is a solution of (5). A steady state $(s_1^*, x_1^*, s_2^*, x_2^*)$ of (4) corresponds to a steady state (s_2^*, x_2^*) of (10) where either $(s_1(t), x_1(t)) = E_0$ or $(s_1(t), x_1(t)) = E_1$. Therefore (s_2^*, x_2^*) must be a steady state of the system

$$\begin{cases} \dot{s}_2 = D(s_2^{in*} - s_2) - f_2(s_2)x_2, \\ \dot{x}_2 = [f_2(s_2) - D_2]x_2 \end{cases} \quad (11)$$

where

$$s_2^{in*} = s_2^{in} \text{ or } s_2^{in*} = s_2^{in} + \frac{D_1}{D}x_1^*. \quad (12)$$

The first case corresponds to $(s_1^*, x_1^*) = E_0$ and the second to $(s_1^*, x_1^*) = E_1$.

The system (11) corresponds to a classical chemostat model with Haldane-type kinetics, including a mortality term for x_2 and an input substrate concentration depending on the input flow rate. The behavior of such a system is well-know, see [4]. A steady state (s_2^*, x_2^*) must be a solution of the system

$$\begin{cases} 0 = D(s_2^{in*} - s_2) - f_2(s_2)x_2, \\ 0 = [f_2(s_2) - D_2]x_2. \end{cases} \quad (13)$$

From the second equation we deduce that $x_2^* = 0$, which correspond to the washout $F_0 = (s_2^{in*}, 0)$ or s_2^* must satisfy the equation

$$f_2(s_2) = D_2. \quad (14)$$

In general, by the hypothesis **A2**, and if we suppose

$$D_2 < f_2(s_2^M) \quad (15)$$

this equation has two solutions such that $s_2^1 < s_2^2$. Therefore the system has two positive steady states $F_1 = (s_2^1, x_2^{1*})$ and $F_2 = (s_2^2, x_2^{2*})$, where

$$x_2^{i*} = \frac{D}{D_2}(s_2^{in*} - s_2^i), \quad i = 1, 2. \quad (16)$$

For $i = 1, 2$, the steady states F_i exist if and only if $s_2^{in*} > s_2^i$.

Proposition 2.2. *Assume that assumptions **A1**, **A2** and (15) hold. Then, the local stability of steady states of (11) is given by :*

1. F_0 is LES if and only if $s_2^{in*} < s_2^1$ or $s_2^{in*} > s_2^2$.
2. F_1 is LES if and only if $s_2^{in*} > s_2^1$ (stable if it exists).
3. F_2 is unstable if it exists (unstable if $s_2^{in*} > s_2^2$).

Proof

The Jacobian matrix of the system (11) is written as follows

$$J = \begin{bmatrix} -D - f_2'(s_2)x_2 & -f_2(s_2) \\ f_2'(s_2)x_2 & f_2(s_2) - D_2 \end{bmatrix}. \quad (17)$$

- For $F_0 = (s_2^{in*}, 0)$, the Jacobian matrix reads

$$J_{F_0} = \begin{bmatrix} -D & -f_2(s_2^{in*}) \\ 0 & f_2(s_2^{in*}) - D_2 \end{bmatrix}.$$

The eigenvalues of J_{F_0} are $\lambda_1 = -D$ and $\lambda_2 = f_2(s_2^{in*}) - D_2$. For being LES, we need $\lambda_2 < 0$ that is to say $f_2(s_2^{in*}) < D_2$. Therefore by **A2** F_0 is LES if and only if $s_2^{in*} < s_2^1$ or $s_2^{in*} > s_2^2$.

- For $F_1 = (s_2^1, x_2^{1*})$, the Jacobian matrix reads

$$J_{F_1} = \begin{bmatrix} -D - f_2'(s_2^1)x_2^{1*} & -D_2 \\ f_2'(s_2^1)x_2^{1*} & 0 \end{bmatrix}.$$

Then we have

$$\begin{aligned} Tr(J_{F_1}) &= -D - f_2'(s_2^1)x_2^{1*} < 0, \\ det(J_{F_1}) &= D_2 f_2'(s_2^1)x_2^{1*} > 0, \end{aligned}$$

therefore, F_1 is LES if it exists.

- For $F_2 = (s_2^2, x_2^{2*})$, the Jacobian matrix reads

$$J_{F_2} = \begin{bmatrix} -D - f_2'(s_2^2)x_2^{2*} & -D_2 \\ f_2'(s_2^2)x_2^{2*} & 0 \end{bmatrix}.$$

Then $det(J_{F_2}) = D_2 f_2'(s_2^2)x_2^{2*}$ is negative, hence the equilibrium F_2 is unstable because the eigenvalues are of opposite signs. This completes the proof of the proposition.

The results are summarized in the following table

Steady-state	Existence condition	Stability condition
F_0	Always exists	$s_2^{in*} < s_2^1$ or $s_2^{in*} > s_2^2$
F_1	$s_2^{in*} > s_2^1$	Stable if it exists
F_2	$s_2^{in*} > s_2^2$	Unstable if it exists

Operating diagram

The operating diagram shows how the system behaves when we vary the two control parameters s_2^{in*} and D . The operating diagram is shown in Fig. (3). The conditions $s_2^{in*} = s_2^1$ or $s_2^{in*} = s_2^2$ are equivalent to $f_2(s_2^{in*}) = D_2$, that is to say $D = \frac{1}{\alpha}(f_2(s_2^{in*}) - k_2)$. Therefore, the horizontal line

$$\Gamma_1 : \left\{ (s_2^{in*}, D) : D = \frac{1}{\alpha}(f_2(s_2^M) - k_2), s_2^{in*} > s_2^M \right\}$$

together with the curve

$$\Gamma_2 : \left\{ (s_2^{in*}, D) : D = \frac{1}{\alpha}(f_2(s_2^{in*}) - k_2) \right\}$$

separate the operating diagram plane in three regions as defined in Fig. (3).

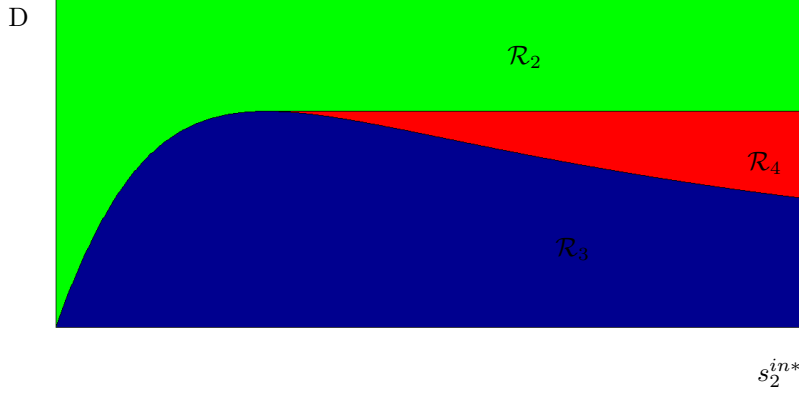


Figure 3: Operating diagram of (11)

The following table indicates the stability properties of steady states in each region.

Region	F_0	F_1	F_2
$(s_2^{in*}, D) \in \mathcal{R}_2$	S		
$(s_2^{in*}, D) \in \mathcal{R}_3$	U	S	
$(s_2^{in*}, D) \in \mathcal{R}_4$	S	S	U

2.3. Steady state of (4)

The aim of this section is to study the dependance of the steady state of (4) with respect to the operating parameters D , s_1^{in} and s_2^{in} . Let $(s_1^*, x_1^*, s_2^*, x_2^*)$ be a steady state of (4), then (s_1^*, x_1^*) is a steady state of (5) and (s_2^*, x_2^*) is a steady state of (11) with (12).

If $(s_1^*, x_1^*) = E_0 = (s_1^{in}, 0)$ then $s_2^{in*} = s_2^{in}$ and three possibilities can occur

1. $(s_2^*, x_2^*) = (s_2^{in}, 0)$, and we denote $E_1^0 := (s_1^{in}, 0, s_2^{in}, 0)$.
2. $(s_2^*, x_2^*) = (s_2^1, x_2^1)$, and we denote $E_1^1 := (s_1^{in}, 0, s_2^1, x_2^1)$
3. $(s_2^*, x_2^*) = (s_2^2, x_2^2)$, and we denote $E_1^2 := (s_1^{in}, 0, s_2^2, x_2^2)$.

If $(s_1^*, x_1^*) = E_1 = (s_1^*, x_1^*)$ then three others possibilities can occur

1. $(s_2^*, x_2^*) = (s_2^{in*}, 0)$, and we denote $E_2^0 := (s_1^*, x_1^*, s_2^{in*}, 0)$.
2. $(s_2^*, x_2^*) = (s_2^1, x_2^{1*})$, and we denote $E_2^1 := (s_1^*, x_1^*, s_2^1, x_2^{1*})$.
3. $(s_2^*, x_2^*) = (s_2^2, x_2^{2*})$, and we denote $E_2^2 := (s_1^*, x_1^*, s_2^2, x_2^{2*})$.

We summarize the results obtained in the previous sections in the following proposition.

Proposition 2.3. *The system (4) has at most six steady states :*

- $E_1^0 = (s_1^{in}, 0, s_2^{in}, 0)$, always exists.
- $E_1^1 = (s_1^{in}, 0, s_2^1, x_2^1)$, exists if and only if $s_2^{in} > s_2^1$.
- $E_1^2 = (s_1^{in}, 0, s_2^2, x_2^2)$, exists if and only if $s_2^{in} > s_2^2$.
- $E_2^0 = (s_1^*, x_1^*, s_2^{in*}, 0)$, exists if and only if $f_1(s_1^{in}, 0) > D_1$.
- $E_2^1 = (s_1^*, x_1^*, s_2^1, x_2^{1*})$, exists if and only if $f_1(s_1^{in}, 0) > D_1$ and $s_2^{in*} > s_2^1$.
- $E_2^2 = (s_1^*, x_1^*, s_2^2, x_2^{2*})$, exists if and only if $f_1(s_1^{in}, 0) > D_1$ and $s_2^{in*} > s_2^2$.

2.4. Stability of steady states of (4)

Now we will study the stability of the steady states given in the Proposition (2.3). For this we consider the Jacobian matrix

$$J = \begin{bmatrix} J_{11} & J_{12} \\ 0 & J_{22} \end{bmatrix},$$

where J_{11} is defined in (8) and J_{22} is defined in (17). This matrix has a block-triangular structure. Hence, the eigenvalues of J are the eigenvalues of J_{11} and the eigenvalues of J_{22} .

The existence of steady states depend only on the relative positions of the two numbers s_1^{in} and s_1^* defined by (7) and of the four numbers s_2^1, s_2^2 defined by (14), s_2^{in} and s_2^{in*} solutions of (12). Equilibria stability is given in the following table.

Table 1: The stability conditions for the system (4)

Equilibria	Evaluated matrices J_{11} and J_{22}	Conditions of stability
E_1^0	$J_{11} = \begin{bmatrix} -D & -f_1(s_1^{in}, 0) \\ 0 & f_1(s_1^{in}, 0) - D_1 \end{bmatrix}$ $J_{22} = \begin{bmatrix} -D & -f_2(s_2^{in}) \\ 0 & f_2(s_2^{in}) - D_2 \end{bmatrix}$	$Tr(J_{11}) < 0 \text{ if } f_1(s_1^{in}, 0) < D_1, \det(J_{11}) > 0$ $Tr(J_{22}) < 0 \text{ if } s_2^{in} < s_2^1 \text{ ou } s_2^{in} > s_2^2, \det(J_{22}) > 0$ $\Rightarrow \begin{cases} E_1^0 \text{ is stable if } f_1(s_1^{in}, 0) \leq D_1 \text{ and} \\ (s_2^{in} < s_2^1 \text{ or } s_2^{in} > s_2^2), \\ E_1^0 \text{ is unstable if } f_1(s_1^{in}, 0) > D_1 \text{ or} \\ s_2^1 < s_2^{in} < s_2^2. \end{cases}$
$E_1^i, i=1,2$	$J_{11} = \begin{bmatrix} -D & -f_1(s_1^{in}, 0) \\ 0 & f_1(s_1^{in}, 0) - D_1 \end{bmatrix}$ $J_{22} = \begin{bmatrix} -[D + f_2'(s_2^i)x_2^i] & -D_2 \\ f_2'(s_2^i)x_2^i & 0 \end{bmatrix}$	$Tr(J_{11}) < 0 \text{ and } \det(J_{11}) > 0 \text{ if } f_1(s_1^{in}, 0) < D_1$ $Tr(J_{22}) < 0 \text{ and } \det(J_{22}) > 0 \text{ at } E_1^1, \det(J_{22}) < 0 \text{ at } E_1^2$ $\Rightarrow \begin{cases} E_1^1 \text{ is stable,} \\ E_1^2 \text{ is unstable} \\ E_1^i \text{ are both unstable if } s_1^{in} > s_1^*. \end{cases}$
E_2^0	$J_{11} = \begin{bmatrix} -[D + (\frac{\partial f_1}{\partial s_1})x_1^*] & -[D_1 + (\frac{\partial f_1}{\partial x_1})x_1^*] \\ (\frac{\partial f_1}{\partial s_1})x_1^* & (\frac{\partial f_1}{\partial x_1})x_1^* \end{bmatrix}$ $J_{22} = \begin{bmatrix} -D & -f_2(s_2^{in*}) \\ 0 & [f_2(s_2^{in*}) - D_2] \end{bmatrix}$	$Tr(J_{11}) < 0 \text{ and } \det(J_{11}) > 0 \text{ by A1}$ $Tr(J_{22}) < 0 \text{ and } \det(J_{22}) > 0 \text{ if } s_2^{in*} < s_2^1 \text{ or } s_2^{in*} > s_2^2$ $\Rightarrow \begin{cases} E_2^0 \text{ is stable if } s_1^{in} \geq s_1^* \text{ and} \\ (s_2^{in*} < s_2^1 \text{ or } s_2^{in*} > s_2^2), \\ E_2^0 \text{ is unstable if } s_1^{in} > s_1^* \text{ and} \\ s_2^1 < s_2^{in*} < s_2^2. \end{cases}$
$E_2^i, i=1,2$	$J_{11} = \begin{bmatrix} -[D + (\frac{\partial f_1}{\partial s_1})x_1^*] & -[D_1 + (\frac{\partial f_1}{\partial x_1})x_1^*] \\ (\frac{\partial f_1}{\partial s_1})x_1^* & (\frac{\partial f_1}{\partial x_1})x_1^* \end{bmatrix}$ $J_{22} = \begin{bmatrix} -[D + f_2'(s_2^i)x_2^{i*}] & -D_2 \\ f_2'(s_2^i)x_2^{i*} & 0 \end{bmatrix}$	$Tr(J_{11}) < 0 \text{ and } \det(J_{11}) > 0$ $Tr(J_{22}) < 0 \text{ and } \det(J_{22}) > 0 \text{ at } E_2^1, \det(J_{22}) < 0 \text{ at } E_2^2$ $\Rightarrow \begin{cases} E_2^1 \text{ is stable,} \\ E_2^2 \text{ is unstable} \end{cases}$

These results are summarized in the following tables, where S and U read for LES and unstable respectively and no letter means that the steady state does not exist.

Table 2: The three cases when $s_1^{in} < s_1^*$

Case	Area	Condition	E_1^0	E_1^1	E_1^2	E_2^0	E_2^1	E_2^2
1.1	\mathcal{A}_1	$s_2^{in} < s_2^1 < s_2^2$	S					
1.2	\mathcal{A}_2	$s_2^1 < s_2^{in} < s_2^2$	U	S				
1.3	\mathcal{A}_3	$s_2^1 < s_2^2 < s_2^{in}$	S	S	U			

Table 3: The six cases when $s_1^{in} > s_1^*$

Case	Area	Condition	E_1^0	E_1^1	E_1^2	E_2^0	E_2^1	E_2^2
2.1	\mathcal{A}_4	$s_2^{in} < s_2^{in*} < s_2^1 < s_2^2$	U			S		
2.2	\mathcal{A}_5	$s_2^{in} < s_2^1 < s_2^{in*} < s_2^2$	U			U	S	
2.3	\mathcal{A}_6	$s_2^{in} < s_2^1 < s_2^2 < s_2^{in*}$	U			S	S	U
2.4	\mathcal{A}_7	$s_2^1 < s_2^{in} < s_2^{in*} < s_2^2$	U	U		U	S	
2.5	\mathcal{A}_8	$s_2^1 < s_2^{in} < s_2^2 < s_2^{in*}$	U	U		S	S	U
2.6	\mathcal{A}_9	$s_2^1 < s_2^2 < s_2^{in} < s_2^{in*}$	U	U	U	S	S	U

Remarque 2.4. Here we have excluded the limit values in the stability condition (Ex: $s_2^{in} = s_2^1$ or $s_2^{in} = s_2^2$...) These cases are related to the eigenvalues of the Jacobian matrix with a real part equal to 0 and the corresponding states are named non-hyperbolic stationary states. Otherwise, they are named hyperbolic steady states.

The different possible cases of non-hyperbolic equilibria are summarized in the following theorem

Theorem 2.5. If $s_1^{in} < s_1^*$, then we have three subcases

Case	Condition	NH	S	U
1.4	$s_2^{in} = s_2^1 < s_2^2$	$E_1^0 = E_1^1$		
1.5	$s_2^1 < s_2^{in} = s_2^2$	$E_1^0 = E_1^2$	E_1^1	
1.6	$s_2^1 = s_2^2 < s_2^{in}$	$E_1^1 = E_1^2$	E_1^0	

If $s_1^{in} > s_1^*$, then we have nine subcases

Case	Condition	NH	S	U
2.7	$s_2^{in} < s_2^{in*} = s_2^1 < s_2^2$	$E_2^0 = E_2^1$		E_1^0
2.8	$s_2^{in} < s_2^1 < s_2^2 = s_2^{in*}$	$E_2^0 = E_2^2$	E_2^1	E_1^0
2.9	$s_2^{in} = s_2^1 < s_2^{in*} < s_2^2$	$E_1^0 = E_1^1$	E_2^1	E_2^0
2.10	$s_2^{in} = s_2^1 < s_2^2 < s_2^{in*}$	$E_1^0 = E_1^1$	E_2^1, E_2^0	E_2^2
2.11	$s_2^{in} = s_2^1 < s_2^2 = s_2^{in*}$	$E_1^0 = E_1^1, E_2^0 = E_2^1$	E_2^1	
2.12	$s_2^1 < s_2^{in} = s_2^2 < s_2^{in*}$	$E_1^1 = E_2^2$	E_2^0	E_1^0
2.13	$s_2^1 < s_2^{in} < s_2^2 = s_2^{in*}$	$E_2^0 = E_2^2$	E_2^1	E_1^0, E_1^1
2.14	$s_2^1 < s_2^{in} = s_2^2 < s_2^{in*}$	$E_1^0 = E_2^1$	E_2^0, E_2^1	E_1^0, E_2^2
2.15	$s_2^1 = s_2^2 < s_2^{in} < s_2^{in*}$	$E_1^1 = E_2^1, E_2^1 = E_2^2$	E_2^0	E_1^0

Proof

Let us give the details of the proof in the **case 2.9**. The other cases can be studied similarly. Assume that $s_2^{in} = s_2^1 < s_2^{in*} < s_2^2$, then $x_2^1 = 0$, $x_1^* > 0$ and $x_2^{1*} > 0$ by (16). Therefore (see Proposition 2.3), the system has three equilibria $E_1^0 = E_1^1$, E_2^0 and E_2^1 . Using the linearization, we obtain that E_2^0 and E_2^1 are hyperbolic.

Remarque 2.6. In each case among those cited in the table (2), (3) and the previous Theorem 2.5 we associate a corresponding figure which represents the relative position of the following parameters s_2^1 , s_2^2 , s_2^{in} and s_2^{in*} (see **Appendix**).

3. Simulations

To illustrate our results, we plot what is called the ‘operating diagrams’ in a number of situations for the system (3) under hypothesis **H1** and **H2**. Recall that operating diagram summarizes the existence and the nature of the equilibria of a dynamical system as a function of its input variables. Here, these control inputs are D , S_1^{in} and S_2^{in} . More particularly, we plot either the operating diagrams in the plan $\{S_1^{in}, D\}$ for a fixed value of S_2^{in} or in the plan $\{S_2^{in}, D\}$ for a fixed value of S_1^{in} . All simulations are performed with the following growth functions:

$$\mu_1(S_1, X_1) = \frac{m_1 S_1}{K_1 X_1 + S_1}, \quad \mu_2(S_2) = \frac{m_2 S_2}{\frac{S_2^2}{I} + S_2 + K_2}.$$

The choice of the values of the model parameters is difficult. Here, our objective is not to match a set of data but rather to highlight the most interesting qualitative properties of the model under interest. To do so, most parameters are taken from [3], while others were changed more significantly as I . Indeed, as underlined in [5], inhibition of the second reaction is not visible if original parameters proposed in [3] are used considering reasonable ranges of variations for S_1 and S_2 . With respect to this later, the Haldane parameter I was thus significantly decreased to willingly increase the effect of the inhibition of the growth of X_2 by S_2 . Finally, parameter values used are summarized in the following table

Table 4: Parameters values of the simulation

Parameter	Unit	Nominal value
m_1	d^{-1}	0.5
K_1	g/L	2.1
m_2	d^{-1}	1
I	$mmol/L$	60
K_2	$mmol/L$	24
k_1	d^{-1}	0.1
k_2	d^{-1}	0.06
α	$\in [0, 1[$	0.5
Y_1	g/g	1/25
Y_2	$g/mmol$	1/250
Y_3	$g/mmol$	1/268

To compute the different regions of the operating diagrams, we use the numerical method reported in [5] which the algorithm is recalled hereafter.

3.1. Algorithm for the determination of the operating diagrams

The algorithm is as follows: for each value of input variables chosen on a grid, the equilibria are computed. The eigenvalues of the Jacobian matrix are then calculated for each equilibrium. Finally, according to the conditions of existence and the sign of the real parts of the eigenvalues, a ‘flag’ is assigned to each of the 6 equilibria: ‘S’ for stable, ‘U’ for unstable or nothing if it does not exist. This procedure stops when all the values of the grid $\{S^{in}, D\}$ have been scanned. As a result, we obtain a number of ‘signatures’ composed of sequences of ‘S’, ‘U’ or ‘nothing’ coding for the existence and stability of the equilibria that we group into regions as summarized in the tables at the end of sections 2.1 and 2.2, respectively. This algorithm may be formalized as follows: let N_1, N_2 be two integers in \mathbb{N}^* and $h_1 = \frac{D}{N_1}$ and $h_2 = \frac{S_{in}}{N_2}$ the two iteration steps:

Algorithm 1 Operating diagram

```
for i varying from 1 to  $N_1$  do;  
  for j varying from 1 to  $N_2$ ;  
    determine 6 equilibria of the model  $E_1 \dots E_6$   
    for k varying from 1 to 6 do  
      calculate the jacobian matrix at  $E_k$  ( $J_{E_k}$ )  
      calculate the eigenvalues of ( $J_{E_k}$ )  
      if all (the conditions of existence of  $E_k$  are fulfilled and all real parts of  
        the eigenvalues of ( $J_{E_k}$ ) are non-positive) then  $E_k$  is stable  
      else if all (conditions of existence of  $E_k$  are fulfilled at least one real part of  
        eigenvalue of ( $J_{E_k}$ ) is positive) then  $E_k$  is unstable  
      else  $E_k$  does not exist  
      end if  
    end for (k)  
  end for (j)  
end for (i)
```

3.2. Operating diagrams

In this part we illustrate our results by plotting the operating diagrams and discuss them.

Fig. (4) represents the operating diagram of model (1) in the plan $\{S_1^{in}, D\}$ for a fixed value of S_2^{in} . The regions are defined as follows. \mathcal{A}_1 (in green) is the stability region of the washout E_1^0 , \mathcal{A}_5 (in blue) is the stability region of steady-state E_2^1 , \mathcal{A}_6 (in red) is the bistability region of the steady-states E_2^0 and E_2^1 , and \mathcal{A}_7 (in dark blue) is the stability region of steady-state E_2^1 , the difference between the regions \mathcal{A}_5 and \mathcal{A}_7 being that the equilibrium E_1^1 does not exist in the region \mathcal{A}_5 but exists and is unstable in \mathcal{A}_7 , see tables (2) and (3).

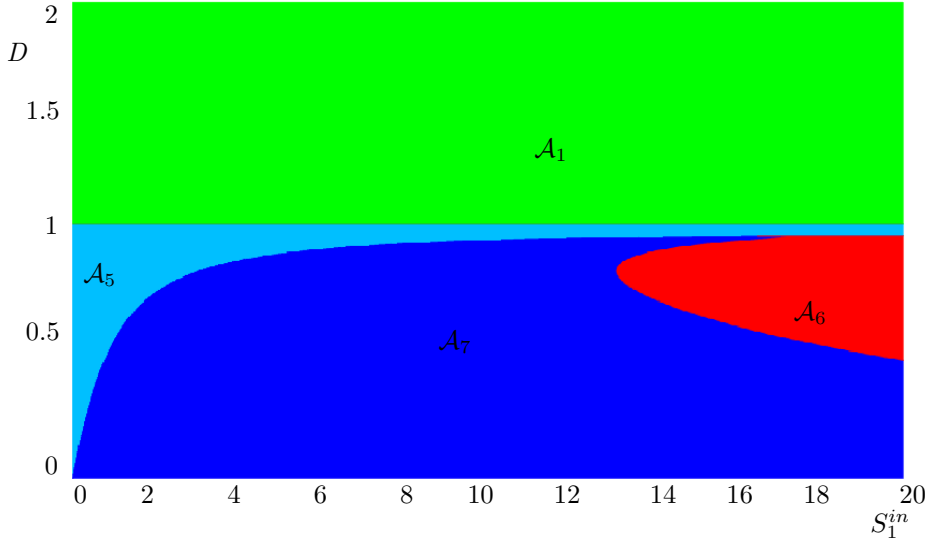


Figure 4: The operating diagram for $S_2^{in} = 1.5 \text{ mmol/L}$.

Fig. (5) represents the operating diagram of model (1) in the plan $\{S_1^{in}, D\}$ for a fixed value of S_2^{in} . The regions are defined as follows. \mathcal{A}_2 (in yellow) is the stability region of steady-state E_1^1 , \mathcal{A}_3 (in orange) is the bistability region of the washout E_1^0 and the steady-state E_1^1 , \mathcal{A}_8 and \mathcal{A}_9 (in pink) and (in dark pink), respectively,

are the bistability regions of the steady-states E_2^0 and E_2^1 , the difference between \mathcal{A}_8 and \mathcal{A}_9 being that the equilibrium E_1^2 does not exist in the region \mathcal{A}_8 but exists and is unstable in \mathcal{A}_9 , see tables (2) and (3).

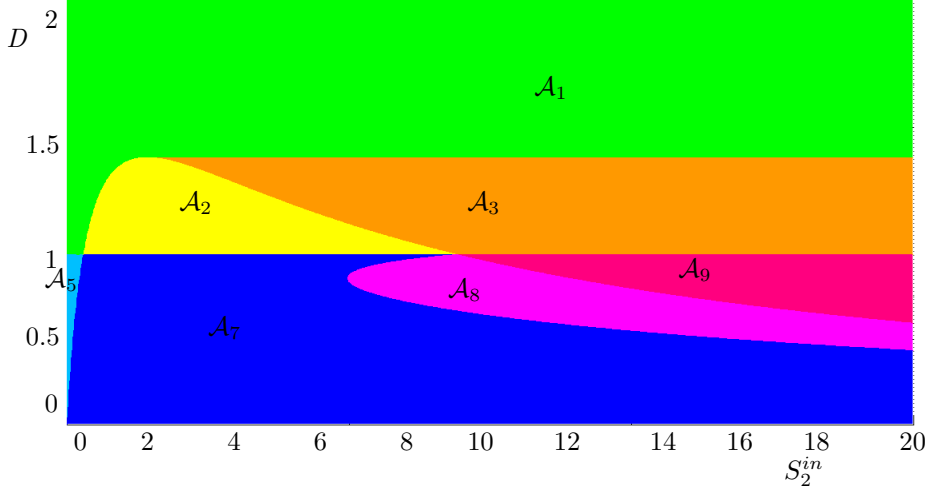


Figure 5: The operating diagram for $S_1^{in} = 0.8 \text{ g/L}$.

Fig. (6) represents the operating diagram of model (1) in the plan $\{S_2^{in}, D\}$ for a fixed but a smaller value of S_1^{in} than before. The differences with the previous case are i) the appearance of a little region \mathcal{A}_4 (in dark orange) which is the stability region of steady-state E_2^0 and ii) a sharp decrease of the size of region \mathcal{A}_8 which almost disappears (it is reduced to a very narrow surface along the frontier with the region \mathcal{A}_9 as can be seen in Fig. (6)).

The region \mathcal{A}_8 becomes very small and narrow compared to Fig. (5) because it is numerically linked to the value of S_1^{in} , that is to say, by reducing the value of S_1^{in} to appear the region \mathcal{A}_4 the size of the region \mathcal{A}_8 is getting smaller and smaller (compare Fig. (5) and (6)). In other words, in decreasing S_1^{in} , the attraction basin of the positive stable equilibrium of \mathcal{A}_7 (E_2^1) increases; it is equivalent to say that, given two values of S_1^{in} , say S_1^{in1} and S_1^{in2} where $S_1^{in2} > S_1^{in1}$, a greater dilution rate is needed to destabilize the process if $S_1^{in} = S_1^{in2}$ than if $S_1^{in} = S_1^{in1}$, thus the sharp decrease of \mathcal{A}_8 observed in Fig. (6).

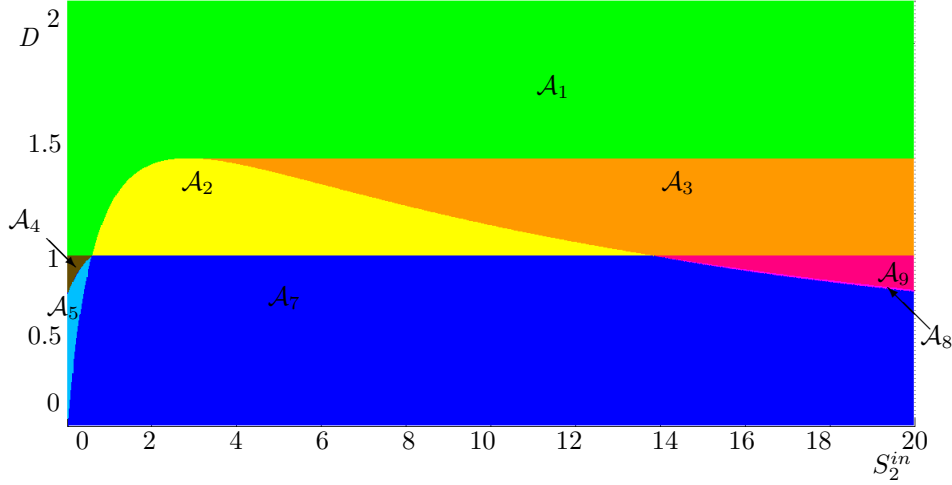


Figure 6: The operating diagram for $S_1^{in} = 0.03 \text{ g/L}$.

3.3. Practical interpretations of the operating diagrams

Herebelow, we explain how the operating diagrams may be used in practice. To illustrate their practical interest, let us consider the operating diagram pictured in Fig. (4) (that is for $S_2^{in} = 1.5 \text{ g/L}$) and let us browse it for increasing values of D at a fixed value of S_1^{in} .

Example 1: Let $S_1^{in} = 18 \text{ g/L}$.

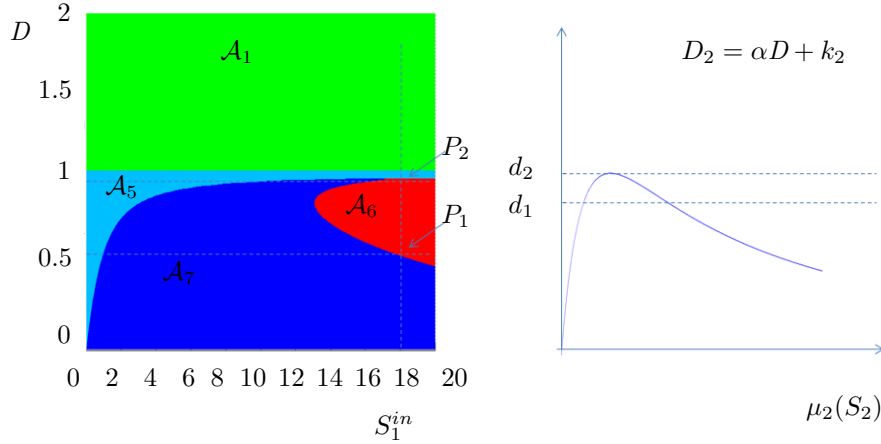


Figure 7: Biological interpretation for $S_1^{in} = 18 \text{ g/L}$

In such a situation, we browse the following regions in considering successive equilibria when increasing D : $\mathcal{A}_7 \rightarrow \mathcal{A}_6 \rightarrow \mathcal{A}_5 \rightarrow \mathcal{A}_1$, see Fig.(7). To better interpret whose ‘steady states the system passes through’, the bifurcation diagram is plotted in Fig. (8).

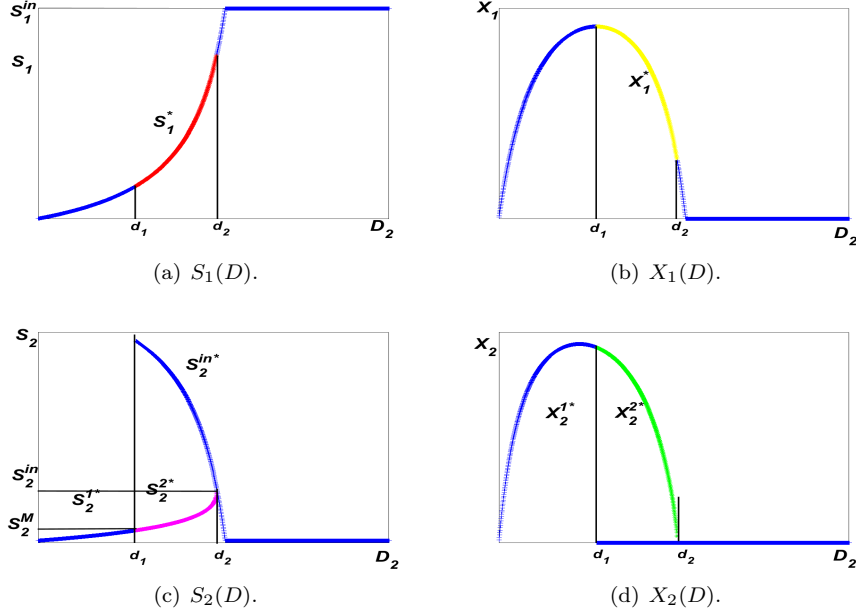


Figure 8: The Bifurcation diagram for the input control D for $S_1^{in} = 18g/L$.

This last diagram allows us to see the appearance/disappearance of steady states as a function of the input variable D (recall that S_1^{in} and S_2^{in} are fixed). As long as D is small enough (i.e. such that $\alpha D + k_2 < d_1$), the quantity of substrate entering the second step of the reaction is very important: the system is in the region \mathcal{A}_7 where the positive equilibrium is the only stable equilibrium. As D increases the size of the attraction basin of this equilibrium decreases until D reaches a critical value (corresponding to the point P_1 in Fig. (7), the frontier between regions \mathcal{A}_7 and \mathcal{A}_6). This critical value corresponds to that one for which the term S_2^{in*} becomes exactly the largest solution of the equation $\mu_2(S_2) = D_2$ (equivalent to equation (14) for the system (4)): the system enters then in the region \mathcal{A}_6 . From a biological point of view, the interpretation is as follows: as D increases, X_1^* decreases and thus S_2^{in*} decreases as can be seen from equation (12). When $D_2 = d_2$, the quantity of available resource necessary to X_2 to grow may become limiting for some initial conditions, leading the system to enter a bistability zone. With the values of the parameters chosen, further increasing D leads definitely X_2 to the washout: the system enters into \mathcal{A}_5 in crossing the point P_2 of Fig. (7). Finally, if D is such that $D_1 = d_2$ (the critical value corresponding to the maximum growth rate of X_1) X_1 goes also to extinction and the system enters into \mathcal{A}_1 .

Example 2: Let $S_1^{in} = 14 g/L$.

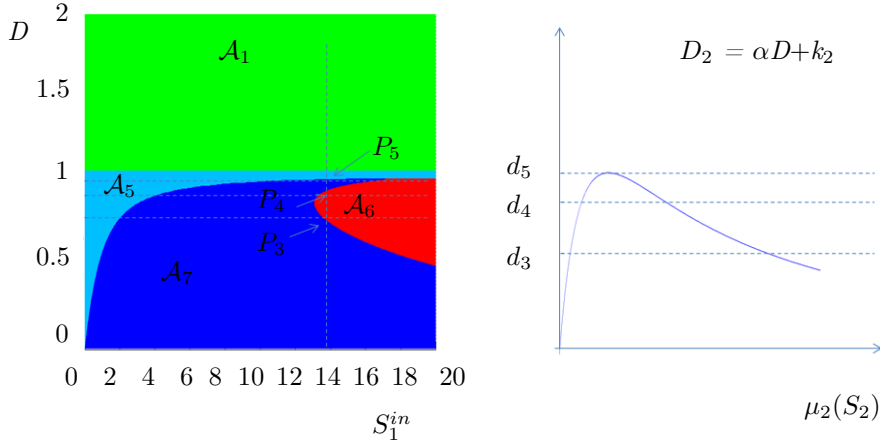


Figure 9: Biological interpretation for $S_1^{in} = 14 \text{ g/L}$

This case is even more interesting since, when D increases, the system goes back to \mathcal{A}_5 once before leaving it definitely in browsing the following regions: $\mathcal{A}_7 \rightarrow \mathcal{A}_6 \rightarrow \mathcal{A}_7 \rightarrow \mathcal{A}_5 \rightarrow \mathcal{A}_1$. While D is small enough (i.e. such that $\alpha D + k_2 < d_3$, cf. Fig. (9)), the reasoning remains the same than before: the only difference is that the value of D leading the system to enter into \mathcal{A}_6 through P_3 is a little bit higher than in the previous case ($d_3 > d_1$). It is due to the fact that the second step of the reaction receives less input from the first step when compared to the case where $S_1^{in} = 18 \text{ g/L}$, thus enlarging the attraction basin of the stable positive equilibrium. Then, when D is further increased, it may happen an interesting phenomenon: the system enters back into \mathcal{A}_7 through point P_4 instead of entering \mathcal{A}_5 as it was the case before. In fact, this strongly depends on model parameters and in particular on the relative rate at which S_2^{in*} and the largest solution of the equation (12) vary as functions of D see Fig. (10). In other words, it depends on how the input concentration of the second step S_2^{in*} - which includes the part of S_1 transformed into S_2 during the first reaction - is affected by D . On the one hand, if we are in a 'flat' zone of the growth rate μ_2 assuming we consider concentrations at the right of the maximum of μ_2 , a small variation of D (and thus of D_2) will change very much the largest solution of the equation (12) while S_2^{in*} may almost remain constant. On the other hand, if D is such that D_2 crosses μ_2 in a sharper zone of the Haldane function (typically around the inflexion point, still considering S_2 evolves at concentrations such as we are on the right of the maximum of μ_2), a small change on D (and thus on D_2) will affect much more the solution of the equation (12) than before. In any of these situations, the relative positions of the largest solution of the equation (12) and of S_2^{in*} determine whether the system will evolve in the region \mathcal{A}_7 or \mathcal{A}_6 and we can observe, as D increases to a value such $\alpha D + k_2 = d_4$ a return of the system from \mathcal{A}_7 into \mathcal{A}_6 through P_3 and then back into \mathcal{A}_7 through P_4 . It is well illustrated in the bifurcation diagram plotted in Fig.(10).

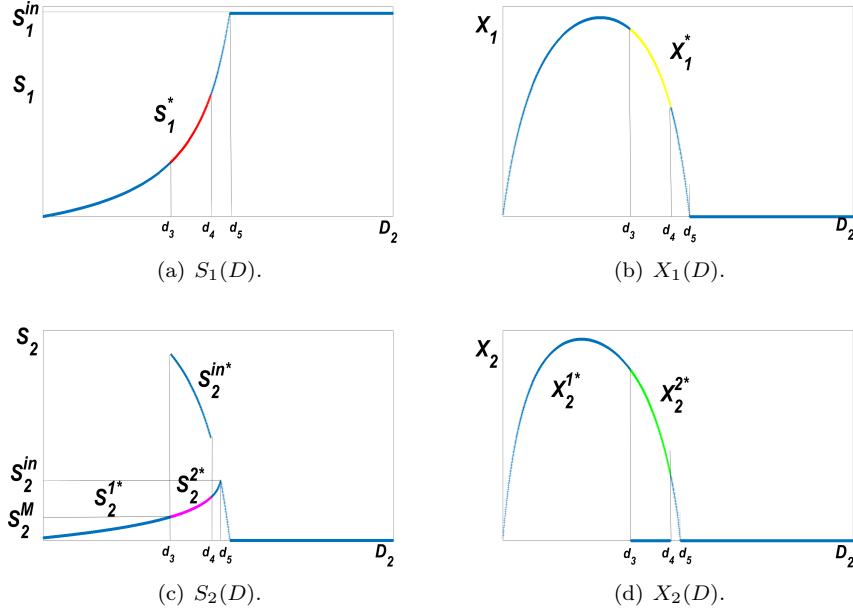


Figure 10: The Bifurcation diagram of the operating diagram show in Fig(4) for $S_1^{in} = 14g/L$.

4. Conclusions

In this paper, we have presented an analysis of an anaerobic digestion model in which we considered two stages corresponding to hydrolysis and methanogenesis phases. We have considered a non usual growth function for hydrolysis step that is the Contois growth function. For the methanogenesis the Haldane law is taken. From the best of authors knowledge, it is the first time such a model including the association of Contois-Haldane growth functions in a two-steps model of the anaerobic digestion is considered. In this analysis we have shown that this model has six steady states $(E_1^0, E_1^1, E_1^2, E_2^0, E_2^1, E_2^2)$. Conditions under which they exist and are stable or unstable have been highlighted. We have also presented the regions of stability of these equilibria with the help of the operating diagrams and discussed their practical use in a number of situations.

Acknowledgements

The authors thank the projects PHC TOUBKAL TBK 17/47-36773WE and the TREASURE Euro-Mediterranean research network (www.inra.fr/treasure) for their financial supports.

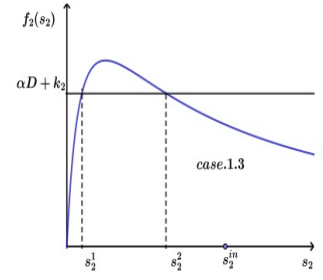
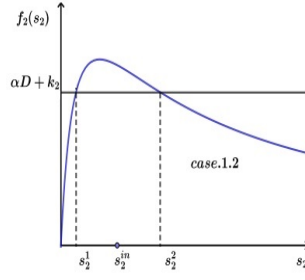
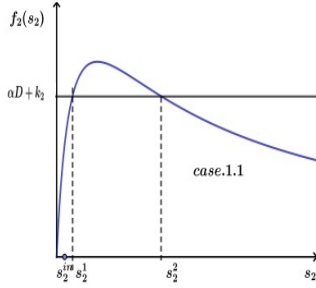
References

- [1] D.J. Batstone, J. Keller, I. Angelidaki, S.V. Kalyzhnyi, S.G. Pavlostathis, A. Rozzi, W.T.M. Sanders, H. Siegrist, V.A. Vavilin (2002). The Iwa Anaerobic Digestion Model No 1 (ADM1). *Water Sci. Technol.* 45, 65-73.

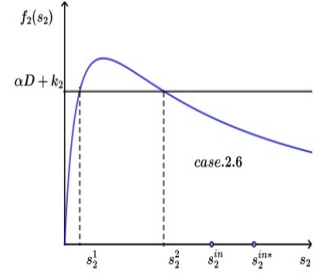
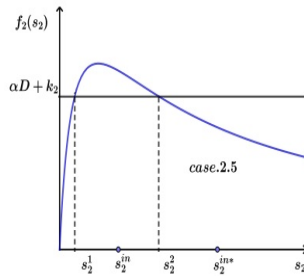
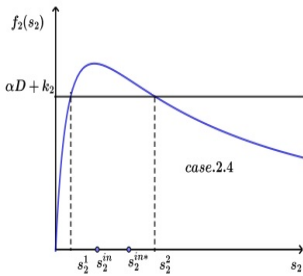
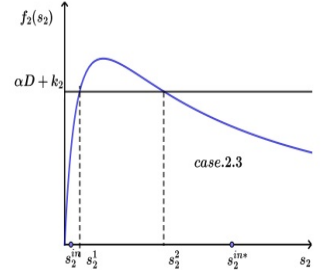
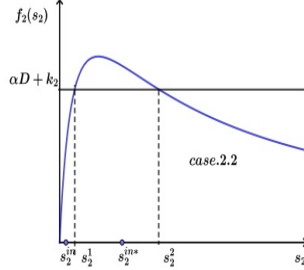
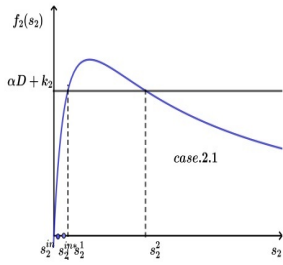
- [2] B. Benyahia, T. Sari, B. Cherki, J. Harmand (2012). Bifurcation and stability analysis of a two step model for monitoring anaerobic digestion processes. *J. Process Control* 22, 1008-1019. doi:10.1016/j.jprocont.2012.04.012
- [3] O. Bernard, Z. Hadj-Sadock, D. Dochain, A. Genovesi, J.-P. Steyer (2001). Dynamical model development and parameter identification for an anaerobic wastewater treatment process. *Biotechnol. Bioeng.* 75, 424-438. DOI: 10.1002/BIT.10036
- [4] J. Harmand, C. Lobry, A. Rapaport, T. Sari (2016), *Chemostat: Theory mathematics of continuous culture of microorganisms*, ISTE.4
- [5] Z. Khedim, B. Benyahia, B. Cherki, T. Sari, J. Harmand (2018), Effect of control parameters on biogas production during the anaerobic digestion of protein-rich substrates, *Applied Mathematical Modelling*, doi: 10.1016/j.apm.2018.04.020.
- [6] I. Ramirez, A. Mottet, H. Carrère, S. Déléris, F. Vedrenne, J.P. Steyer (2009), Modified ADM1 disintegration/hydrolysis structures for modeling batch thermophilic anaerobic digestion of thermally pretreated waste activated sludge, doi:10.1016/j.watres.2009.05.023
- [7] P.J.Reilly (1974). Stability of commensalistic systems. *Biotechnol. Bioeng.* 16, 1373-1392. doi: 10.1002/bit.260161006
- [8] M. Sbarciog, M. Loccufier, E Nolus (2010). Determination of appropriate operating strategies for anaerobic digestion systems. *Biochemical engineering journal* 51 (3), 180-188. doi:10.1016/j.bej.2010.06.016
- [9] T. Sari and J. Harmand (2016). A model of a syntrophic relationship between two microbial species in a chemostat including maintenance. *Mathematical Biosciences* 275, 1-9. doi:10.1016/j.mbs.2016.02.008
- [10] G. Stephanopoulos (1981). The dynamic of commensalism. *Biotechnol. Bioeng.* 23, 2243-2255. doi: 10.1002/bit.260231008
- [11] V.A. Vavilin, B. Fernandez, et al.(2008). Hydrolysis kinetics in anaerobic degradation of particulate organic material: An overview. *Waste Management* 28,939-951. doi:10.1016/j.wasman.2007.03.028
- [12] E.I.P. Volcke, M. Sbarciog, E.J.L. Noldus, B. De Baets, M. Loccufier (2010). Steady-state multiplicity of two-step biological conversion systems with general kinetics. *Mathematical Biosciences* 228, 160-170. doi:10.1016/j.mbs.2010.09.004
- [13] M.J. Wade, J. Harmand, B. Benyahia, T. Bouchez, S. Chailou, B. Arditi, C. Lobry (2016). Perspectives in mathematical modelling for microbial ecology. *Ecological Modelling* 321, 64-74. doi:10.1016/j.ecolmodel.2015.11.002
- [14] M. Weeder mann, G. Wolkowicz, J. Sasara (2015). Optimal biogas production in a model for anaerobic digestion. *Nonlinear Dynamics* 81,1097-1112. doi 10.1007/s11071-015-2051-z
- [15] M. Weeder mann, G. Seo, G. Wolkowics (2013). Mathematical Model of Anaerobic Digestion in a Chemostat: Effects of Syntrophy and Inhibition. *Journal of Biological Dynamics* 7, 59-85. doi:10.1080/17513758.2012.755573

Appendix: The relative positions of the following parameters s_2^1 , s_2^2 , s_2^{in} and s_2^{in*} see [2].

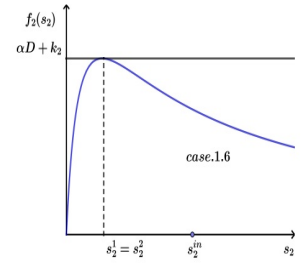
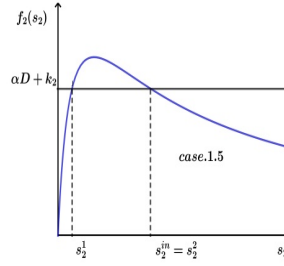
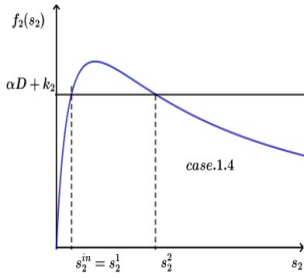
Different cases when $s_1^{in} < s_1^*$



Different cases when $s_1^{in} > s_1^*$



Different cases when $s_1^{in} < s_1^*$



Different cases when $s_1^{in} > s_1^*$

